Journal of Solid State Chemistry **167,** 310–323 (2002)
doi:10.1006/jssc.2002.9631

Study of Ion-Exchanged Microporous Lithosilicate Na–RUB-29 Using Synchrotron X-Ray Single-Crystal Diffraction and ^{6}Li MAS NMR Spectroscopy

So-Hyun Park,* Martin Kleinsorge,*,† Clare P. Grey,† and John B. Parise*,†,[1]

*Department of Geosciences, State University of New York; and †Chemistry Department, at Stony Brook, Stony Brook, New York 11794

Received December 3, 2001; in revised form April 18, 2002; accepted May 2, 2002

DEDICATED TO PROFESSOR GALEN STUCKY ON THE OCCASION OF HIS 65TH BIRTHDAY

Synchrotron X-ray single-crystal diffraction analyses revealed that as-synthesized and Na-exchanged RUB-29 (Cs_{1-x}, $Na_x)_{14}Li_{24}[Si_{72}Li_{18}O_{172}]\cdot yH_2O$ ($x = 0$, 0.9) displays the lattice symmetry *I*222. With increasing ion-exchange time, the Na cations preferentially replace Cs in the larger sites located at the intersections of the 10MR/10MR/8MR channels. The smaller Cs sites are then replaced. While Na cations are easily incorporated on the Cs sites, most of non-framework Li cations remain in the channel system. Relocation of Li cations onto new sites within the channels was observed only after 13 days of ion exchange. Using high-field (14.1 T) NMR spectroscopy, at least six separate ^{6}Li resonances could be resolved for the first time by solid-state ^{6}Li MAS NMR spectroscopy and assigned to Li in the framework and non-framework sites of the microporous lithosilicate materials. The fate of Li in both framework and extra-framework sites during exchange was also followed by ^{6}Li MAS NMR spectroscopy with an Na-exchanged RUB-29 powder sample.

Key Words: **RUB-29; Na–RUB-29; lithosilicate; microporous; zeolite; ion exchange; ^{6}Li MAS NMR; structure; synthesis.**

INTRODUCTION

The recently discovered lithosilicate RUB-29 ($Cs_{14}Li_{24}[Si_{72}Li_{18}O_{172}]\cdot 14H_2O$) possesses a unique topology (Fig. 1) and is a member of a family of new framework structures (1, 2). The open $[Si_{72}Li_{18}O_{172}]$ framework is comprised of corner-shared $[SiO_4]$- and corner and edge-shared $[LiO_4]$-tetrahedra. These structural elements are strictly segregated into alternating layer-like building units (LLBU) which are interconnected to form a three-dimensional system of channels bounded by 3-, 4-, 5-, 6-, 8-, 9-, and 10-membered rings (MR) as shown in Fig. 1. Inclusion of edge-sharing $[LiO_4]$ building units decreases the anion-to-cation ratio in the framework to just below 2.0, the value expected for frameworks with all-corner-connected tetrahedra. Nonetheless, the conceptual substitution of Li for Si in the framework gives rise to a high framework charge, which is balanced by Cs and Li cations in the channels. Because of this high concentration of charge-balancing cations, as-synthesized RUB-29 behaves more like a dense phase in terms of gas diffusion or other materials transport properties within the pore system.

The exchange of the larger channel-blocking ions for smaller cations represents an important first step toward investigating the utility of these new materials for gas separation and catalysis. Results from our initial investigations suggested that at least 60% of the Cs cations were readily exchangeable by Na within 1 h in a 5 M NaCl solution (1). Here we report a more systematic study of the ion-exchange process of RUB-29 and the structural changes that accompany ion exchange of this chemically and structurally complex material.

There are seven unique positions available for Cs cations (labeled Cs1–Cs7 in Fig. 1) and four for the non-framework Li cations (Li4, Li5, Li7, and Li8) in the channels of as-synthesized RUB-29. The ease with which ion-exchange occurs at these sites may depend on their locations, with cations located on larger, more accessible sites being more readily exchanged than those on smaller sites. Details of the crystal structure during the ion-exchange process can help rationalize which sites are available for exchange and the mechanism by which exchange occurs (3–6).

The crystal structure also provides a means to determine the bond strengths at each cation site (7). We are interested in determining the structural consequences of Na exchange

[1] To whom correspondence should be addressed. Fax: +1-631-632-8140. E-mail: sohpark@notes.cc.sunysb.edu or jparise@notes.cc.sunysb.edu.

0022-4596/02 $35.00

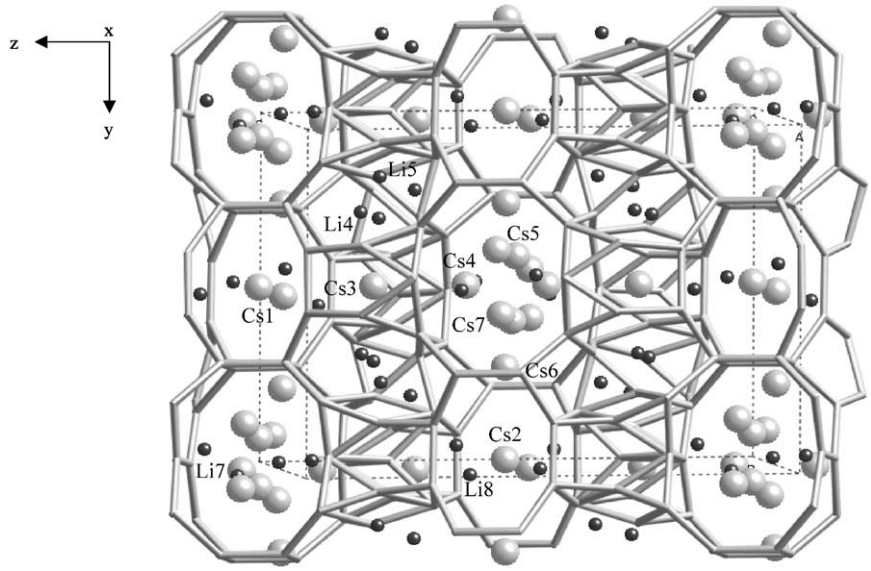

FIG. 1. Location of Cs and Li cations in the three-dimensional channel system of as-synthesized RUB-29. The (001) planes of Si–O and Li–O layer-like building units (LLBU) alternate along [001]. Oxygen sites, at the approximate midpoints of the lines, are omitted for clarity and the Si and Li atoms lie at the nodes of the net.

into RUB-29. In previous studies we have noted that as exchange proceeds, subtle changes in framework geometry can have profound effects on the rate and order in which ions are exchanged (3). We hypothesize that access and bond strength, as determined from crystal structure analysis, might be indicators of how readily a particular site is exchanged. Bond valences (BV) calculated for extra-framework cations using the method of Brown and Shannon (8) were calculated for RUB-29. Cation–oxygen cut-off distances of 4 and 3 Å were considered in the calculation of BV for Cs–O and Li–O, respectively. Based upon the results presented in Table 1, the Cs1 site is expected to be the most difficult to exchange.

Accessibility to the cation sites from the pore system is also important. In the case of exchange into Y-type zeolites for example (3), crystal structure analysis of a series of samples showed access to the double 6-ring is restricted because exchanging cations must first negotiate large pores and sites at single 6-rings. In the case of RUB-29, the Cs1 site, the smallest of all sites for Cs, is located within the 8MR channels parallel to [100], at the middle of a double 8MR and a double 4MR as shown in Fig. 2a. The other Cs sites are shown in Fig. 2 and include a variety of environments. A reasonable starting hypothesis is that Cs and Li cations within the larger channel spaces would be more readily exchanged than those occluded in smaller pores. The thrust of the present work is to test this hypothesis and to characterize changes in the framework geometry, which might affect access to these sites.

Because of the complexity of the RUB-29 structure and our desire to obtain accurate atomic structural information, we employed single-crystal diffraction (XSD) methods. Because of the small size of the crystals (1), and their decrease in size upon exchange, a third-generation synchrotron source was required for data collection. The large number of structural parameters (>330) and the high degree of peak overlap expected for even high-resolution synchrotron XRD, limits the accuracy of powder investigations. Future time-resolved powder investigations also depend on accurate structure determinations for native and fully exchanged materials to provide constraints for Rietveld refinements of the structures of the intermediate exchange steps (3, 4).

While X rays provide sensitivity toward the population of the Cs site, they are relatively insensitive to the populations of the Li sites. Recent studies of Li-bearing zeolitic materials (9, 10) suggest that the location of different Li sites can be probed and the population

TABLE 1

Bond Valence (BV) of Cs Cations in the RUB-29 Structure, Calculated According to the Suggestion of Brown and Shannon $BV = (R/R_O)^{-N}$ with $N = 6.6$ and $R_O = 2.335$ for Cs Cations in Oxides (8)

Cs cation site	BV of Cs within the first coordination sphere
Cs1	0.90
Cs2	0.79
Cs3	0.61
Cs4	0.83
Cs5	0.57
Cs6	0.35
Cs7	0.77

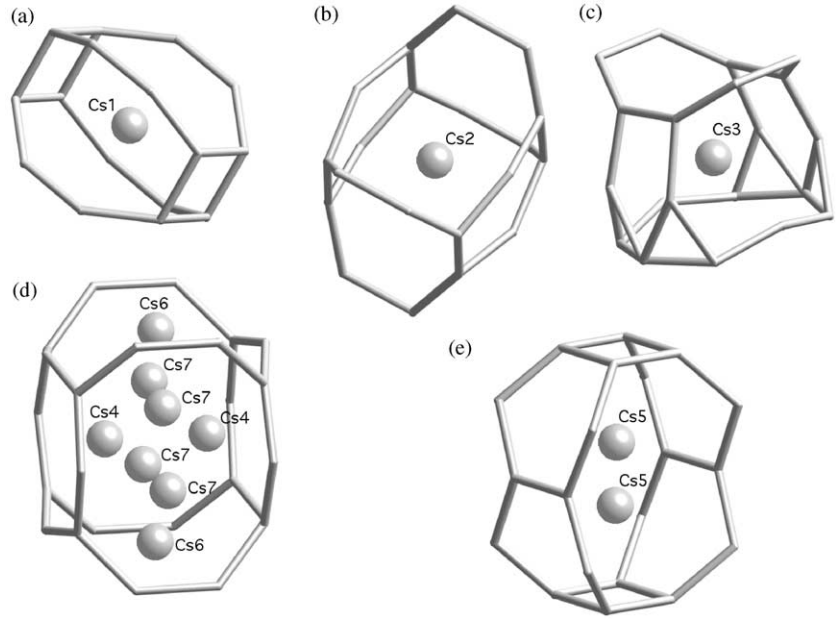

FIG. 2. Pore spaces for sites occupied by Cs^+ within RUB-29: (a) Cs1, (b) Cs2, (c) Cs3, (d) channel spaces for Cs4, Cs6, and Cs7, and (e) Cs5. The lines represent *T*–O–*T* connections (*T* = Li or Si) with oxygen, at the approximate midpoint of the lines, omitted for clarity.

determined quantitatively by using ^{6}Li and ^{7}Li MAS NMR spectroscopy. In particular, the location of the Li cations impacts directly on nitrogen absorption properties of the materials due to a strong interaction between Li cations and nitrogen molecules (11). Stebbins and his collaborators (12) observed multiple Li cation sites of Li_4SiO_4 and its substituted derivatives such as $Li_{4.1}Al_{0.1}Si_{0.9}O_4$ and $Li_{3.7}Al_{0.1}SiO_4$ and estimated their exchange rate with increasing temperature using high-resolution ^{6}Li MAS NMR techniques. Feuerstein and Lobo investigated zeolite LiLSX (Li-exchanged low-silica X) using ^{6}Li and ^{7}Li MAS NMR in combination with neutron diffraction analysis (13). The three resolved ^{7}Li resonances of the dehydrated form of the material were assigned to three Li cation sites (SI′, SII, and SIII) located at different channel positions. With oxygen-loaded LiLSX samples, they also observed a shift of one of the resonances to higher frequency. This resonance was assigned to cations in site SIII and the shift was attributed to the interaction of the paramagnetic molecules with this site (14).

While NMR is a sensitive tool for the determination of Li mobility and site population, all attempts to distinguish non-framework and framework Li cation sites in microporous lithosilicates by ^{6}Li- and ^{7}Li NMR spectroscopy to date were unsuccessful (1, 15, 16). The ^{6}Li- and ^{7}Li spectra displayed only one resonance at around 0 ppm and a series of low-temperature experiments with dehydrated microporous lithosilicate samples (from 0°C to −150°C) did not improve the resolution, even when oxygen was loaded into samples (16). In this paper, we show that the ^{6}Li resolution is dramatically improved by the use of high field strengths (14.1 T), even without the use of oxygen loading. The shifts observed upon sodium ion exchange were used to help distinguish between the peaks of the framework Li and those of the non-framework Li cations in the ^{6}Li MAS NMR spectra of RUB-29 and Na–RUB-29.

EXPERIMENTAL SECTION

Synthesis of RUB-29

A pure RUB-29 sample was made by using the optimized synthesis parameters reported in detail in Ref. (2). We have modified the preparations somewhat by applying a long aging time. After preparing a reaction mixture with the molar composition $1SiO_2$:$0.23Li_2O$:$0.23Cs_2O$:0.08TEAOH:$40H_2O$, the resulting gel was aged for 5 days at room temperature with slow stirring. The gel became a highly basic, water-clear solution and was charged into 23 mL Teflon-lined stainless autoclaves (Parr). The hydrothermal synthesis was carried on within a convection oven for 7 days at 220°C. A mass synthesis was carried out by using 120 mL Teflon vessels to produce a high amount of pure RUB-29 for NMR and ion-exchange experiments with powder samples. In this case, the synthesis time increased to 10 days, from 7 days, to maximize the crystallization gain. The crystalline product contains only RUB-29 with no impurities. For ^{6}Li MAS NMR experiments, $^6LiOH \cdot H_2O$ (98% ^{6}Li, Aldrich) was used in the synthesis gel as an Li source.

Preparation of Na–RUB-29

A 5 M aqueous NaCl solution was chosen to minimize the ion-exchange time and sample hydrolysis. Twenty glass vials with a volume of 3 mL were filled with 5 M NaCl solution, and about 10 mg of RUB-29 crystals added to each. All were kept at room temperature and were shaken sporadically. From that batch, one vial per day of Na-exchanged RUB-29 crystals was carefully washed with deionized water and dried at room temperature (RT). This, in principle, provided 20 different degrees of Na exchange. The samples were designated according to exchange time, with Na1d being a sample of Na–RUB-29 obtained by Na exchanging for 1 day, Na2d for 2 days, and so on.

To produce a well-exchanged and high-quality powder sample for ^{6}Li MAS NMR spectra of Na–RUB-29, 4 g of as-synthesized RUB-29 was finely ground and ion exchanged in 100 mL of 5 M NaCl solution while stirring gently for 30 min. The powder sample was washed with deionized water and dried at RT overnight. This exchange treatment was repeated on this sample twice. This sample is designated Na-3–RUB-29 (powder). For chemical analysis, 1 g of Na-3–RUB-29 (powder) was sent to Galbraith Laboratories, Inc., Knoxville, TN, USA.

TABLE 2
Summary of the Results of Crystallographic Experiments and the Structure Refinements of Na–RUB-29 Na1d, Na5d, Na13d, and Na18d with Increasing Degree of Na Exchange

	Na1d	Na5d	Na13d	Na18d
Lattice parameter a (Å)	11.216(2)	11.160(2)	11.177(2)	11.156(2)
Lattice parameter b (Å)	17.360(1)	17.264(4)	17.354(6)	17.356(4)
Lattice parameter c (Å)	23.916(5)	23.969(5)	24.203(4)	24.137(5)
Space group	$I\,222$	$I\,222$	$I\,222$	$I\,222$
Wavelength (Å)	0.6199	0.6199	0.6199	0.6199
Scan mode	$\varpi - 2\theta$	$\varpi - 2\theta$	$\varpi - 2\theta$	$\varpi - 2\theta$
Exposure time/frame (s)	5	2	15	10
2θ range (°)	51.83	62.93	51.81	51.95
Number of unique reflections after merging for Fourier	3431	4583	3682	3493
$R_1(= \Sigma\|\|F_o\| - \|F_c\|\|/\Sigma\|F_o\|)$ for all unique reflections	0.04	0.16	0.10	0.09
Good of fit (χ^2)[a]	1.1	1.1	1.6	1.6
Number of Cs, Na, and Li cations in an idealized structure formula $(Cs,Na,Li)_{38}[Si_{72}Li_{18}]\cdot xH_2O$	Cs = 6.4 Na = 10.7 Li = 20.9	Cs = 6.4 Na = 10.8 Li = 20.8	Cs = 3.7 Na = 14.1 Li = 20.2	Cs = 1.2 Na = 16.6 Li = 20.2

[a] $\chi 2 = \Sigma w(|F_o|^{2-}|F_c|^2)^2/(N - P)$, where N is the number of observations, P is the number of variable parameters, and w is the weight $(= 1/[\sigma^2(F_o^2) + (0.2p)^2 + 0.0p]$ with $p = (\mathrm{Max}(F_o^2, 0) + 2F_c^2)/3)$.

Synchrotron X-Ray Diffraction

Data collection for the crystallographic data of Na1d, Na5, Na13d, and Na18d was conducted at beam line 13BMD of the GeoSoilEnviro Consortorium for Advanced Radiation Science (GSE-CARS) of the Advanced Photon Source (APS) of Argonne National Laboratory. Each Na–RUB-29 crystal with a edge length between 20 and 30 μm was mounted and data were collected on a Bruker charge coupled device (CCD) detector with a graphite monochromator [$\lambda = 0.6199(3)$ Å]. The crystal is located at a distance of 3.92 cm from the detector and rotated about 360° continually during the data collection in the $\varpi/2\theta$ scan mode. The integrated reflections were corrected for the absorption effect using the program SADABS, distributed by Bruker Analytical (17). The crystal structures were solved by direct methods, and then refined by difference Fourier calculations with SHELXTL of the Bruker program suite (17). Table 2 summarizes experimental conditions and results for the data collected on each sample.

Solid-State ^{6}Li High-Power Decoupling Magic Angle Spinning Nuclear Magnetic Resonance (HPDEC MAS NMR) Spectroscopy

As-synthesized RUB-29 and Na-3–RUB-29 (powder) samples were ground and packed into 4 mm rotors. The amount of both samples was 0.1524 and 0.1289 g, respectively. Solid-state ^{6}Li HPDEC MAS NMR spectra were acquired using a Bruker Advance 600 spectrometer with a Larmor frequency 88.32 MHz for ^{6}Li. For the experiments, an H/X double-resonance MAS probe was used with a spinning rate of 10 kHz. The spectra were acquired with an ^{6}Li pulse width of 2.2 μs and a pulse delay of 300 s. Proton decoupling was applied to remove the ^{6}Li–^{1}H heteronuclear coupling by applying an RF power strength of 83 kHz for ^{1}H. ^{6}Li spectra were referenced to 1 M ^{6}LiOH solution at 0 ppm, as an external reference. For the quantitative analysis of peak intensities, the same scan number of 16 was used for the acquisition of all the spectra.

RESULTS AND DISCUSSION

Analysis of Synchrotron X-Ray Single-Crystal Diffraction Data

All single-crystal XRD data collected at the APS for the Na-exchanged samples Na1d, Na5d, Na13d, and Na18d were consistent with the space group of the as-synthesized (native) RUB-29, *I*222. The chemical composition of each exchanged sample was determined directly from the refinement results.

The initial structure models for all samples were determined from direct methods, which revealed the positions for atoms in the $[Si_{72}O_{176}]$ building unit and several extra-framework sites for cesium (Cs1–Cs4). Fourier difference calculations revealed two sites occupied by

sodium, located sites close to Cs7 and Li7 found in as-synthesized RUB-29 (1, 2). Subsequent full matrix least-squares refinement established the site occupancies for the Cs and Na sites, with the isotropic displacement parameters (U_{iso}) for these sites constrained to a value of $0.05\,\text{Å}^2$. This value was chosen from the mean for the sites occupied by Cs and water molecules in the native RUB-29 (1, 2). All these Cs and Na sites are less than 100% occupied, consistent with static disorder of the channel constituents and their statistical occupancy of multiple closely spaced sites. Because of this, it is likely that these sites are partially occupied and/or are multiply occupied by a mixture of, for example, ($Cs + H_2O$). A precise determination of site chemistry is therefore difficult based upon X-ray diffraction data alone. Even with appropriate chemical constraints, ambiguity because of similarities in scattering power can cause confusion. For example, it is not possible to differentiate between occupancies of (0.35 Cs + 0.65 Na) vs (0.3 Cs + 0.4 Na + 0.3 H_2O) since both these occupancies result in a similar scattering. This will give rise to an occupancy parameter of 50% Cs when the site is refined for a Cs position. Clearly supplemental data from neutron powder diffraction might help here, although difficulties in duplicating the same exchange and hydration state in powder and single crystal would complicate analysis in this case.

All Li positions in the framework, Li1–Li3, and Li6, along with two non-framework positions, Li4 and Li5, were located at more advanced stages of the structural study, and after a reasonable convergence on the populations of the sites occupied by Cs, Na and water was achieved. Two of the other Cs sites (Cs5, Cs6) and one channel Li cation site (Li8) found in the as-synthesized RUB-29 structure did not appear in the difference electron density maps generated at this stage. In the last refinement cycles for Na13d and Na18d, however, a new site for non-framework Li cations was found, located at about $z = +0.5$ from the Li8 position in the native material (2). In addition, in the Na18d structure, a new position for Li was found in the vicinity of Cs6 (2). The occupancies of these Li sites were refined using displacement parameters constrained to $0.025\,\text{Å}^2$ chosen from the mean for the Li sites in the original RUB-29 refinement (1, 2). The results of crystallographic refinements for samples Na1d and Na5d, Na13d, and Na18d are summarized in Table 2. Detailed crystallographic data are available from the authors upon request.

Effect of Na Exchange on the Framework Structure

The longer the exposure to the exchange solution the greater the amount of Cs replaced in the extra-framework sites. The amount of Cs exchange is 91% and 54% for Na18d and Na1d, respectively. In response, the lattice parameters for Na–RUB-29 would be expected to decrease with increasing exchange of the larger Cs^+ by the smaller Na^+. While the unit cell parameter a is reduced from Na1d to Na18d (Fig. 3a), the unit cell parameter c increases (Fig. 3c). There is also an increase in the lattice parameter b and the cell volume from Na5d to Na13d (Fig. 3b and 3d and Table 2).

Since the degree of Na exchange occurring on the Li sites varied only from 13% (Na1d and Na5d) to 16% (Na13d and Na18d), the replacement of Li^+ by the larger of Na^+ alone cannot explain expansion of the lattice along [001]. Changes in hydration level as exchange proceeds and mixed occupancy by water of cation sites in the channels may also be important. To determine the importance of this effect, studies of dehydrated Na–RUB-29 using neutron powder diffraction data are in progress.

Subtle and, sometimes, dramatic changes in framework geometry accompany ion exchange (18, 19). Careful consideration of these changes often provides clues to the mechanism of the exchange process (3, 4). Seeking the root structural cause of the unusual behavior of the framework during exchange of Cs^+ for Na^+, we compare selected bond lengths and angles for the primary building units, the TO_4 ($T = \text{Si, Li}$) tetrahedra, and the interconnections between them, for Na1d and Na18d in Tables 3 and 4. There is no systematic trend in all these geometrical parameters to indicate a structural origin for the lattice parameter expansion parallel to [001] (Fig. 3). More subtle local changes in the secondary building units (SBU) were then considered.

The RUB-29 framework (Fig. 1) contains two layer-like building units (LLBUs), one containing edge- and corner-linked [LiO_4] moieties and one of corner-connected [SiO_4] tetrahedra. Their interconnection creates (Li, Si)-spiro-5- and (Li, Si)-spiro-3,5-building units shown in Fig. 4. These building units consist of [(Si, Li)] tetrahedra with the center of each of them occupied exclusively by lithium (1, 2). This geometry, unique in microporous materials, probably results from the capability of lithium to build geometrically flexible tetrahedra with oxygen atoms. Given its flexibility we hypothesized this unusual SBU could be responsible for the abnormal expansion of the Na–RUB-29 lattice in the [001] direction with increasing Na exchange.

The [LiO_4] LLBUs are positioned parallel to (001) so that the longer side of all (Li, Si)- spiro-5- and (Li, Si)-spiro-3,5-building units are arranged parallel to each other perpendicular to the (001) lattice plane (Fig. 1). Therefore, the bonding angles at the center of each (Li, Si)-spiro-5- and (Li, Si)-spiro-3,5-building unit can impact the changes in the lattice parameter c. Based upon this consideration, we focused on finding any systematic changes in the $\angle$(O–Li–O) angles of Na18d from those of Na1d framework. With reference to Fig. 4 and the discussion below, the following changes in angle are abstracted from Table 3 and represented schematically in Fig. 4. In the

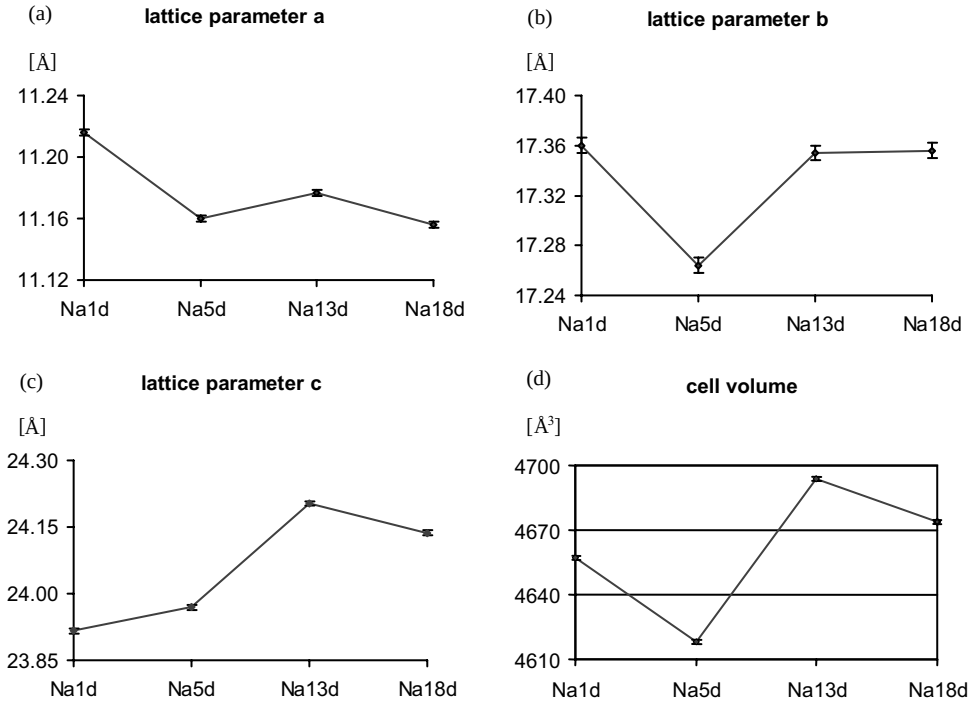

FIG. 3. Changes in lattice parameters *a* (a), *b* (b), *c* (c), and cell volume (d) upon Na exchange of the single-crystal RUB-29 samples Na1d, Na5d, Na13d, and Na18d.

(Li1,Si)-spiro-3,5 SBU: $\angle$(O21–Li1–O1) = 101.0° → 101.8° and $\angle$(O21*–Li1–O1*) = 100.9 → 101.8°; in (Li6,Si)-spiro-3,5: $\angle$(O13–Li6–O21) = 99.7° → 109.0° and $\angle$(O3–Li6–O15) = 97.6° → 92.4°; in (Li2,Si)-spiro-5: $\angle$(O5–Li2–O1) = 116.8 → 125.0° and $\angle$(O21–Li2–O13) = 109.7° → 101.8°; in (Li3,Si)-spiro-5: $\angle$(O9–Li3–O15) = 103.1° → 104.8° and $\angle$(O21–Li3–O1) = 95.2° → 97.2°.

As shown in Fig. 4, the increase in the $\angle$(O–Li–O) angles parallel to the *c*-axis for (Li1, Si)-spiro-3,5 (Fig. 4a) and the (Li3, Si)-spiro-5 (Fig. 4b) of Na18d causes a stretching in [001]. In the cases of (Li6, Si)-spiro-3,5 (Fig. 4a) and (Li2, Si)-spiro-5 (Fig. 4b), only one side of each spiro-3,5- and spiro-5-building unit become enlarged whereas the opposite side of each is reduced. Nevertheless, from Na1d to Na18d, the degree of enlargement of the angles $\angle$(O–Li–O) at the center of (Li6, Si)-spiro-3,5 and of (Li2, Si)-spiro-5 are bigger than the reduced values (Fig. 4b). As a result, both building units are also stretched in the [001] direction. Based on these observations, the expansion of the lattice parameter *c* appears to be restricted to changes in [LiO_4] at the center of the spiro-SBU.

Details of Na Exchange on the Cs Cation Sites

In the native RUB-29 structure, the Cs1 site is located at the middle of a double 8MR and a double 4MR (Fig. 2a) as mentioned. The Cs2 site is located at the intersection of the 10MR- (∥[010]) and the 8MR-channels (∥[100]). The double 10MR bounding the Cs2 site is connected via a double 8MR (Fig. 2b). The Cs3 site is a big cage-like pore space with 8MR- and 9MR openings within the layer-like building units of the [LiO_4] tetrahedra parallel to the lattice plane (001) (Fig. 2c). The Cs4-, Cs6-, and Cs7 sites are present in the largest channel space, located at the intersection of 10MR- (∥[100]), 10MR- (∥[010]), and 8MR-channels (∥[001]) (Fig. 2d). The Cs5 site is built within double 10MR, two double 6MR, and a double 4MR within 10MR channels parallel to [100] forming a big pore space (Fig. 2e). As a result, the space volume of the Cs5 site is bigger than that of Cs2 and Cs3.

The composition of the non-framework sites changes continually during Na exchange. After 18 days, more than 85% of cesium in sites Cs2–Cs4, and Cs7 was replaced by Na (Table 5). As expected from arguments based upon bond valence (Table 1) only 42% Cs cations on Cs1, which is the smallest channel void available for Cs in RUB-29, was exchanged by Na. The most readily exchanged sites (Fig. 5 and Table 1) generally have lower bond valence sums.

In order to compare the relative exchange of Na into the seven Cs sites, the occupancies of these positions were recalculated (Table 6) and are shown in Fig. 5, assuming that all possible Cs sites were occupied only by Cs cations. The results for the actual refinement are also reported in Table 5 with the types of scattering factor chosen for modeling occupancy parameters of each non-framework

TABLE 3
Bonding Distances and Angles within the Na1d and Na18d Na–RUB-29 Framework Structures

Na1d–RUB-29					Na18d–RUB-29				
Central atom	Atom	Bond length (Å)	Angle (°)		Central atom	Atom	Bond length (Å)	Angle (°)	
Si1	O22	1.626(5)	O22–Si1–O1	113.6(3)	Si1	O22	1.636(7)	O22–Si1–O1	113.8(4)
	O1	1.594(3)	O22–Si1–O12	104.9(2)		O1	1.583(4)	O22–Si1–O12	106.5(3)
	O12	1.624(2)	O22–Si1–O20	104.9(2)		O12	1.614(2)	O22–Si1–O20	105.0(2)
	O20	1.632(5)	O1–Si1–O12	114.8(2)		O20	1.624(6)	O1–Si1–O12	113.7(2)
			O1–Si1–O20	112.8(3)				O1–Si1–O20	112.2(4)
			O12–Si1–O20	104.9(2)				O12–Si1–O20	104.9(3)
Si2	O5	1.596(5)	O5–Si2–O4	113.5(2)	Si2	O5	1.589(7)	O5–Si2–O4	114.1(3)
	O4	1.633(6)	O5–Si2–O11	112.1(3)		O4	1.654(8)	O5–Si2–O11	111.4(4)
	O11	1.625(5)	O5–Si2–O18	114.2(3)		O11	1.606(8)	O5–Si2–O18	112.6(4)
	O18	1.648(5)	O4–Si2–O11	108.7(2)		O18	1.600(8)	O4–Si2–O11	107.4(4)
			O4–Si2–O18	102.4(2)				O4–Si2–O18	103.1(3)
			O11–Si2–O18	105.2(3)				O11–Si2–O18	107.5(4)
Si3	O8	1.612(5)	O8–Si3–O10	107.9(2)	Si3	O8	1.585(6)	O8–Si3–O10	108.1(3)
	O10	1.562(6)	O8–Si3–O18	112.2(3)		O10	1.608(9)	O8–Si3–O18	111.3(4)
	O18	1.602(5)	O8–Si3–O2	108.9(2)		O18	1.628(7)	O8–Si3–O2	110.3(3)
	O2	1.631(6)	O10–Si3–O18	109.0(2)		O2	1.622(1)	O10–Si3–O18	109.6(3)
			O10–Si3–O2	109.2(2)				O10–Si3–O2	109.6(3)
			O18–Si3–O2	109.6(3)				O18–Si3–O2	108.1(4)
Si4	O3	1.570(3)	O3–Si4–O17	110.6(3)	Si4	O3	1.564(4)	O3–Si4–O17	109.8(4)
	O17	1.628(5)	O3–Si4–O6	114.6(1)		O17	1.634(7)	O3–Si4–O6	113.8(2)
	O6	1.629(3)	O3–Si4–O19	113.0(3)		O6	1.632(4)	O3–Si4–O19	115.9(4)
	O19	1.623(5)	O17–Si4–O6	108.6(3)		O19	1.595(7)	O17–Si4–O6	108.1(4)
			O17–Si4–O19	103.2(2)				O17–Si4–O19	102.2(3)
			O6–Si4–O19	106.1(3)				O6–Si4–O19	106.2(4)
Si5	O13	1.611(5)	O13–Si5–O20	112.8(3)	Si5	O13	1.596(8)	O13–Si5–O20	113.5(4)
	O20	1.635(4)	O13–Si5–O7	110.8(3)		O20	1.651(6)	O13–Si5–O7	111.1(4)
	O7	1.645(5)	O13–Si5–O19	116.6(3)		O7	1.615(7)	O13–Si5–O19	111.6(8)
	O19	1.622(6)	O20–Si5–O7	107.0(3)		O19	1.652(8)	O20–Si5–O7	105.9(4)
			O20–Si5–O19	103.9(3)				O20–Si5–O19	103.7(4)
			O7–Si5–O19	105.0(3)				O7–Si5–O19	105.2(4)
Si6	O9	1.575(5)	O9–Si6–O16	112.1(3)	Si6	O9	1.570(7)	O9–Si6–O16	115.3(6)
	O16	1.630(5)	O9–Si6–O14	112.6(3)		O16	1.675(6)	O9–Si6–O14	112.7(4)
	O14	1.645(6)	O9–Si6–O4	114.0(2)		O14	1.658(7)	O9–Si6–O4	114.1(3)
	O4	1.626(6)	O16–Si6–O14	108.6(3)		O4	1.595(8)	O16–Si6–O14	106.1(4)
			O16–Si6–O4	102.2(2)				O16–Si6–O4	102.2(3)
			O14–Si6–O4	106.7(2)				O14–Si6–O4	105.4(3)
Si7	O17	1.621(5)	O17–Si7–O8	108.0(3)	Si7	O17	1.608(6)	O17–Si7–O8	107.5(4)
	O8	1.605(5)	O17–Si7–O15	107.4(4)		O8	1.631(6)	O17–Si7–O15	109.5(5)
	O15	1.549(6)	O17–Si7–O22	103.3(3)		O15	1.568(7)	O17–Si7–O22	102.5(4)
	O22	1.637(5)	O8–Si7–O15	115.1(3)		O22	1.631(6)	O8–Si7–O15	115.1(4)
			O8–Si7–O22	105.6(3)				O8–Si7–O22	106.1(4)
			O15–Si7–O22	116.7(3)				O15–Si7–O22	115.1(4)
Si8	O21	1.589(3)	O21–Si8–O14	111.8(3)	Si8	O21	1.581(4)	O21–Si8–O14	113.7(4)
	O14	1.629(6)	O21–Si8–O6	110.8(2)		O14	1.631(7)	O21–Si8–O6	111.4(2)
	O6	1.624(3)	O21–Si8–O11	114.6(3)		O6	1.618(4)	O21–Si8–O11	111.9(4)
	O11	1.646(5)	O14–Si8–O6	109.1(3)		O11	1.642(7)	O14–Si8–O6	109.3(4)
			O14–Si8–O11	104.3(2)				O14–Si8–O11	103.6(2)
			O6–Si8–O11	105.9(3)				O6–Si8–O11	106.4(4)

TABLE 3—*Continued*

Na1d–RUB-29					Na18d–RUB-29				
Central atom	Atom	Bond length (Å)	Angle (°)		Central atom	Atom	Bond length (Å)	Angle (°)	
Si9	O2	1.606(6)	O2–Si9–O10	109.3(2)	Si9	O2	1.598(10)	O2–Si9–O10	110.0(3)
	O10	1.637(6)	O2–Si9–O7	110.0(2)		O10	1.580(9)	O2–Si9–O7	109.1(4)
	O7	1.573(5)	O2–Si9–O16	109.3(2)		O7	1.580(7)	O2–Si9–O16	109.3(3)
	O16	1.619(5)	O10–Si9–O7	109.4(2)		O16	1.583(6)	O10–Si9–O7	109.3(3)
			O10–Si9–O16	109.0(2)				O10–Si9–O16	107.7(3)
			O7–Si9–O16	110.0(3)				O7–Si9–O16	111.5(4)
Li1	O21	1.962(4)	O21–Li1–O21[a]	134.5(5)	Li1	O21	1.950(6)	O21–Li1–O21[a]	137.8(8)
	O21[a]	1.962(4)	O21–Li1–O1	101.0(2)		O21[a]	1.950(6)	O21–Li1–O1	101.8(3)
	O1	1.925(5)	O21–Li1–O1[a]	100.3(2)		O1	1.941(7)	O21–Li1–O1[a]	98.4(3)
	O1[a]	1.925(5)	O21[a]–Li1–O1	100.3(2)		O1[a]	1.941(7)	O21[a]–Li1–O1	98.4(3)
			O21[a]–Li1–O1[a]	100.9(2)				O21[a]–Li1–O1[a]	101.8(3)
			O1–Li1–O1[a]	122.8(5)				O1–Li1–O1[a]	121.5(7)
Li2	O21	1.97(1)	O21–Li2–O5	114.7(6)	Li2	O21	2.08(2)	O21–Li2–O5	111.3(9)
	O5	1.93(1)	O21–Li2–O13	109.7(6)		O5	1.92(2)	O21–Li2–O13	101.8(8)
	O13	1.92(1)	O21–Li2–O1	97.1(5)		O13	2.01(2)	O21–Li2–O1	95.8(8)
	O1	2.01(1)	O5–Li2–O13	108.5(6)		O1	1.89(2)	O5–Li2–O13	108.3(9)
			O5–Li2–O1	116.8(6)				O5–Li2–O1	125.0(10)
			O13–Li2–O1	109.6(5)				O13–Li2–O1	111.4(9)
Li3	O9	1.93(1)	O9–Li3–O1	127.0(6)	Li3	O9	1.94(2)	O9–Li3–O1	120.4(12)
	O1	1.90(1)	O9–Li2–O15	103.1(5)		O1	2.00(2)	O9–Li2–O15	104.8(11)
	O15	1.99(1)	O9–Li2–O21	108.9(5)		O15	1.92(2)	O9–Li2–O21	112.2(11)
	O21	2.12(1)	O1–Li2–O15	114.4(5)		O21	2.03(2)	O1–Li2–O15	113.2(11)
			O1–Li2–O21	95.2(4)				O1–Li2–O21	97.2(10)
			O15–Li2–O21	105.4(5)				O15–Li2–O21	108.6(11)
Li6	O15	2.16(2)	O15–Li6–O3	97.6(7)	Li6	O15	2.28(2)	O15–Li6–O3	92.4(8)
	O3	1.95(1)	O15–Li6–O21	102.3(7)		O3	2.02(2)	O15–Li6–O21	98.1(8)
	O21	2.04(1)	O15–Li6–O13	149.1(5)		O21	1.97(1)	O15–Li6–O13	146.1(8)
	O13	2.13(2)	O3–Li6–O21	111.4(5)		O13	1.93(2)	O3–Li6–O21	110.2(7)
			O3–Li6–O13	94.2(7)				O3–Li6–O13	96.9(8)
			O21–Li6–O13	99.7(7)				O21–Li6–O13	109.0(9)

[a] Symmetrically equivalent.

site shown beside their position names. The occupancy of the Cs4 site, one of the larger Cs sites with a high bond valence (Table 1) and jointly occupied by Cs and water, steadily increased from Na1d to Na13d (Table 6 and Fig. 5). This result, which requires verification perhaps by characterization of dehydrated Na–RUB-29 samples, indicates that there may be an induction period over which no exchange occurs on this site while other larger Cs sites are preferentially exchanged. In the final stage of ion exchange over 18 days, Cs cations on the Cs4 site were also almost completely exchanged by Na, as shown in the Na18d structure (Table 5).

The Cs5 and Cs6 sites found in the structure of the native material (1, 2) show particularly low bond valence sums (Table 1). The sites are occupied by neither Na nor Cs in Na–RUB-29. Surprisingly, structural analysis of the single-crystal data of Na18d revealed an Li cation site nearby the Cs6, which will be discussed in the following section in more detail.

Effect of Na Exchange on the Li Cation Sites

As shown in Fig. 1, the Li4 and Li5 sites are located in small pore voids within $[LiO_4]$-layer-like building units, where the nature of the framework necessitates the highest charge balance per unit volume, because of the compactly localized framework $[LiO_4]$ tetrahedra in the RUB-29 structure (1, 2). Therefore, it was expected that the larger sodium might find it difficult to replace these non-framework Li cations. Compared to Li4 and Li5, the two other sites for non-framework Li cations (Li7 and Li8) could be available for Na exchange because these are located in the large channel spaces. The Li7 site was found in the vicinity

TABLE 4
Comparison of (*T*–O–*T*) Bonding Angles within the RUB-29 Framework to Those within Na–RUB-29 Structures, Na1d and Na18d

(*T*–O–*T*)	Bonding angle (°) within RUB-29 (as-synthesized)	Bonding angle (°) within Na–RUB-29 (Na1d)	Bonding angle (°) within Na–RUB-29 (Na18d)
Si1–O1–Li1(, –Li2, –Li3)	116.2(9) [; 115.399); 122.2(10)]	113.0(3) [; 118.1(4); 117.2(4)]	113.5(4) [; 120.2(7); 114.8(8)]
Si1–O12–Si1[a]	141.1(7)	141.6(3)	144.0(4)
Si1–O20–Si5	133.6(7)	132.9(3)	133.2(4)
Si1–O22–Si7	130.6(7)	133.4(4)	134.2(5)
Si2–O4–Si6	142.2(4)	142.3(2)	142.3(2)
Si2–O5–Li2	118.1(9)	115.8(5)	115.3(7)
Si2–O11–Si8	134.3(6)	133.9(4)	136.5(5)
Si2–O18–Si3	132.6(6)	134.5(3)	137.9(5)
Si3–O2–Si9	136.4(4)	139.8(2)	144.5(3)
Si3–O8–Si7	144.1(8)	149.2(3)	150.0(5)
Si3–O10–Si9	151.4(4)	154.4(2)	157.6(3)
Si3–O18–Si2	132.6(6)	134.5(3)	137.9(5)
Si4–O3–Li6	119.0(7)	119.7(3)	123.8(8)
Si4–O6–Si8	142.5(4)	142.6(2)	142.1(3)
Si4–O17–Si7	136.2(9)	137.5(4)	138.3(5)
Si4–O19–Si5	136.9(8)	137.5(4)	137.5(5)
Si5–O7–Si9	147.3(6)	148.6(3)	151.0(5)
Si5–O13–Li2 (, Li6)	111.4(9) [; 122.6(8)]	113.9(4) [; 133.4(5)]	108.3(6) [; 139.0(7)]
Si5–O19–Si4	136.9(8)	137.5(4)	137.5(5)
Si5–O20-Si1	133.6(7)	132.9(3)	133.2(4)
Si6–O4–Si2	142.2(4)	142.3(2)	142.3(2)
Si6–O9–Li3	116.3(13)	116.2(4)	116.1(8)
Si6–O14–Si8	131.9(6)	134.1(4)	131.5(5)
Si6–O16–Si9	130.5(6)	134.9(3)	136.0(4)
Si7–O8–Si3	144.1(8)	149.2(3)	150.0(5)
Si7–O15–Li3(, –Li6)	110.4(11) [; 138.3(9)]	110.7(4) [; 125.8(6)]	113.7(8) [; 127.2(7)]
Si7–O17–Si4	136.2(9)	137.5(4)	138.3(5)
Si7–O22–Si1	130.6(7)	133.4(4)	134.2(5)
Si8–O6–Si4	142.5(4)	142.6(2)	142.1(3)
Si8–O11–Si2	134.3(6)	133.9(4)	136.5(5)
Si8–O14–Si6	131.9(6)	134.1(4)	131.5(5)
Si8–O21–Li1(, –Li2, –Li3, –Li6)	129.3(9) [; 114.0(9); 111.3(12); 119.7(7)]	128.7(3) [; 111.2(5); 120.8(3); 113.4(4)]	125.9(4) [; 112.5(8); 111.5(8); 122.6(5)]
Si9–O2–Si3	136.4(4)	139.8(2)	144.5(3)
Si9–O7–Si5	147.3(6)	148.6(3)	151.0(5)
Si9–O10–Si3[a]	151.4(4)	154.4(2)	157.6(3)
Si9–O16–Si6	130.5(6)	134.5(3)	136.0(4)

[a] Symmetrically equivalent.

of Cs4 and Cs7 while the Li8 is at the corner of the double 10MR of the Cs2 site (Fig. 1). As shown in Fig. 2, the pore space for the Li7 site is larger than that for the Li8.

The occupancy of sites Li4 and Li5 did not change within the precision provided by the structure refinement and indicates that Na^+ does not replace Li^+ at these sites. The bond valences (7, 8) for the Li4 and Li5 sites, 0.81 and 0.87, respectively, are comparable to those for the Li6 site in the framework, 0.86. These are weaker than those for the other three framework Li cation sites, Li1, Li2, and Li3 with valence sums of 1.06, 0.98, and 0.99, respectively. They are however higher than that for Li7 (0.70). The occupancy value for this site, located in 10MR channels, increases continuously from Na1d through Na18d, with most of Li^+ replaced by Na^+. In Table 7, nearest bonding distances between the Li7 site and oxygen atoms are given to show a correlation of these distances with the degree of Na exchange on the Li7 site between RUB-29 and Na–RUB-29. With increased exchange degree, the distances *d*(Li7–O) increase. This fact is consistent with the observation that the Li7 site within Na18d is occupied by more Na cations (and water molecules) than in Na1d.

In Na–RUB-29 structures investigated so far, we could not find lithium cations in the Li8 site. The site was determined to be a channel Li cation site in the as-synthesized RUB-29 structure by using neutron powder diffraction data (1). Instead of the Li8 site, a new Li site designated $Li8^*$ was found in Na13d and Na18d. This is located about $z = +0.5$ from the position of Li8 parallel to the *c*-axis. The occupancy of $Li8^*$ (0.6) is similar to that of Li8 in RUB-29.

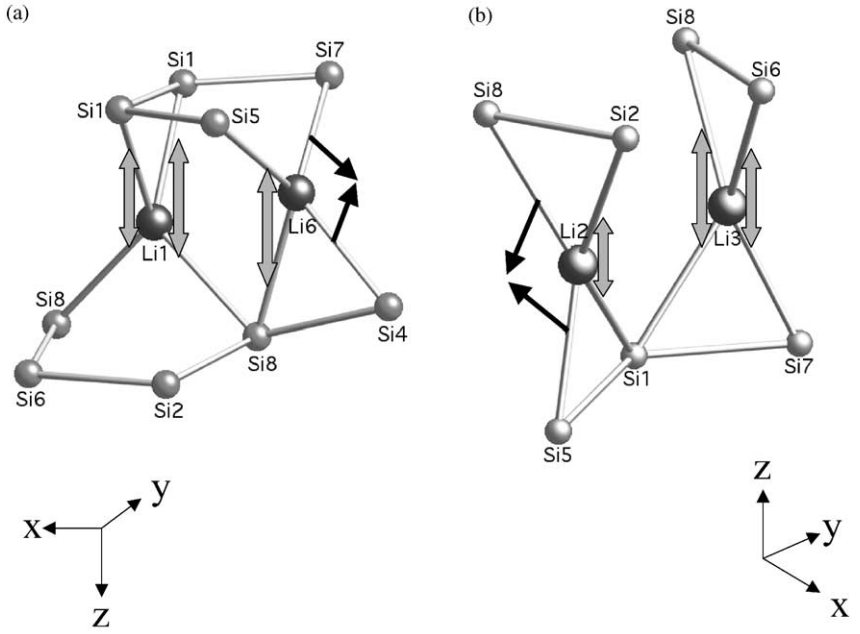

FIG. 4. Schematic representation of the changes occurring in bond angle (Table 3) in the (Li, Si)-spiro-3,5- (a) and (Li, Si)-spiro-5 building units (b). These changes result in a stretching of the units parallel to the [001] direction within the framework of Na–RUB-29. Small circles indicate the centers of $[SiO_4]$ tetrahedra and big circles those of $[LiO_4]$ tetrahedra, and oxygen sites are omitted for clarity.

As mentioned above, the Cs5 and Cs6 sites found in the native form of RUB-29 are occupied by neither Na nor Cs in Na–RUB-29. Analysis of the single-crystal data for Na18d, however, revealed a new special position, which might be occupied by Li. The new site is located near Cs6, and their similarity suggests that lithium cations may also occupy the Cs5 site. To test this possibility is non-trivial using X-ray diffraction data because of the low scattering power of lithium. In the case of Na–RUB-29, the situation is more problematic because most of these small Li cations are present in the vicinity of heavy Cs cations disordered with Na and water molecules. Despite these difficulties, the analysis of data performed from Na18d suggests that Li cations are located nearby the Cs6 site. The result may be due, however, to a small amount of Cs cations remaining in Na18d (9%), present only on the Cs1 site located far from possible Li cation sites. Regarding the dramatic change in occupancies on the Cs5, Cs6, and Li8 sites of Na–RUB-29 from those of RUB-29 (Fig. 5), it is clear that lithium prefers to relocate while cesium is exchanged by sodium.

TABLE 5
Summary of Occupancy Parameters on Non-framework Cation Sites of As-Synthesized RUB-29 and Four Different Na–RUB-29 structures

	Atom type for calculations of occupancy and resulting occupancy value of each non-framework cation site									
Site name	As-synthesized RUB-29		Na–RUB-29 Na1d		Na–RUB-29 Na5d		Na–RUB-29 Na13d		Na–RUB-29 Na18d	
Cs1	Cs	1.00(1)	Cs	0.93(1)	Cs	0.80(1)	Cs	0.61(1)	Cs	0.58(1)
Cs2	Cs	1.00(1)	Cs	0.70(1)	Cs	0.54(1)	Na	0.66(1)	Na	0.80(3)
Cs3	Cs	1.00(1)	Cs	0.43(1)	Cs	0.48(1)	Na	0.64(2)	Na	0.68(2)
Cs4/H_2O	Cs	0.38(5)	Cs	0.35(2)	Cs	0.47(1)	Cs	0.62(1)	Na	0.58(1)
Cs5/H_2O	Cs	0.48(5)	—	—	—	—	—	—	—	—
Cs6/H_2O	Cs	0.98(4)	—	—	—	—	—	—	Li	0.2(1)
Cs7/H_2O	Cs	0.60(2)	Na	0.37(1)	Na	0.39(2)	Na	0.39(2)	Na	0.41(2)
Li4	Li	1.0(2)	Li	1.0(1)	Li	0.6(1)	Li	0.8(1)	Li	0.7(1)
Li5	Li	0.7(2)	Li	1.0(1)	Li	1.0(1)	Li	0.8(1)	Li	0.8(1)
Li7	Li	0.6(1)	Na	0.39(2)	Na	0.40(2)	Na	0.47(1)	Na	0.46(2)
Li8	Li	0.6(1)	—	—	—	—	Li[a]	0.6(1)	Li[a]	0.6(1)

[a] This site is located about $z = +0.5$ from the original location Li8 parallel to [001]. This indicates a relocation of non-framework Li cations while Na cations exchange Cs.

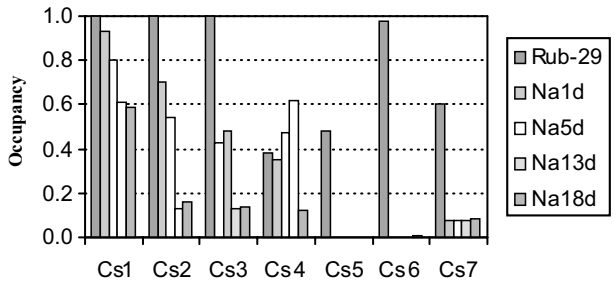

FIG. 5. Schematic of changes in the occupancy values on Cs cation sites of RUB-29 upon Na exchange. For ready comparison, the values were recalculated by hypothesizing that all Cs cites were occupied by Cs cations only. Except for the Cs1 site, Na cations replaced most of Cs sites after 18 days. An increase in occupancy on the Cs4 site following Na ion exchange may indicate that the cations on Cs4 were not exchanged until most of the other large Cs sites were replaced by Na. A new Li cation site, designated Li8*, in the vicinity of Cs6 was determined in the Na18d structure (see text).

TABLE 6
Comparison of Occupancy Parameters on Cs Cation Sites, Assuming that all Possible Cs Sites are Occupied Only by Cs Cations

Site name	RUB-29	Na1d	Na5d	Na13d	Na18d
Cs1(Cs)	1	0.93	0.8	0.61	0.58
Cs2(Cs)	1	0.7	0.54	0.13	0.16
Cs3(Cs)	1	0.43	0.48	0.13	0.14
Cs4(Cs)	0.38	0.35	0.47	0.62	0.12
Cs5(Cs)	0.48				
Cs6(Cs)	0.98				0.01
Cs7(Cs)	0.6	0.074	0.078	0.078	0.082

^{6}Li HPDEC MAS NMR Spectroscopy of As-Synthesized RUB-29 and Na-3–RUB-29 (Powder) and Chemical Analysis

Chemical analysis of the powder sample of Na–RUB-29, Na-3–RUB-29 (powder), was consistent with the structural formula $Cs_6Li_{22}Na_{10}[Si_{72}Li_{18}O_{72}] \cdot xH_2O$. This composition corresponds to an Na–RUB-29 composition in between that of Na5d and Na13d. A total number of Li cations of 42 and 40 for the as-synthesized and Na-3–RUB-29, respectively, was obtained by chemical analysis (Table 8).

Fig. 6 shows the ^{6}Li HPDEC MAS NMR spectra of as-synthesized RUB-29 and Na-3–RUB-29 (powder). The spectra of as-synthesized RUB-29 contains at least six resonances at 1, 0.89, 0.76, 0.41, 0.18, and 0.02 ppm (Fig. 6a) while the Na-exchanged form has only three broad peaks at 0.95, 0.66, and 0.25 ppm (Fig. 6b). This is the first observation of clearly resolved ^{6}Li NMR resonances due to Li cations in porous lithosilicates. The integrated intensities of each resonance were obtained by deconvolution of the spectrum. The intensities of the ^{6}Li NMR resonances of Na-3–RUB-29 were normalized to the sample weight of as-synthesized RUB-29 (Fig. 7 and Table 8).

The resonances at 0.41, 0.18, and 0.02 ppm in the RUB-29 spectrum are no longer resolved in Na–RUB-29. Instead, a broad resonance at 0.25 ppm, corresponding to the same number of cations as the resonances at 0.41–0.02 ppm in the as-synthesized sample, is observed. On this basis, these resonances are assigned to framework, non-exchangeable, Li cations.

A shift to higher frequency for the light element Li is generally indicative of a decrease in shielding. Framework Li are expected to be more shielded than the extra-framework sites, consistent with our assignment of these sites to the resonances from 0.02 to 0.41 ppm. The resonance at 0.02 ppm of RUB-29 is tentatively assigned to the Li1 site, based on its shortest Li–O distances, which result in its highest bond valence of all the framework Li sites. Furthermore, the number of Li cations calculated from the intensity of the resonance at 0.02 ppm is the same number of Li cations on the Li1 site (= 3 per unit cell) obtained from the crystal structure analysis (1). In the same way, the intense resonance at 0.18 ppm of Rub-29 is assigned to framework Li cations on Li2, Li3, and Li6 sites.

The next most clear-cut assignment is the resonance due to Li7. Since most of the lithium cations on the Li7 site of Na–RUB-29 are exchanged by sodium cations, the

TABLE 7
Comparison of Interatomic Distances between the Center of the Li7 Site and the Nearest Oxygen Atoms of As-Synthesized RUB-29 to Those of Na–RUB-29 Structures Na1d and Na18d

As-synthesized RUB-29		Na–RUB-29 (Na1d)		Na–RUB-29 (Na18d)	
Vector	Length (Å)	Vector	Length (Å)	Vector	Length (Å)
Li7–O20	2.45(11)	Li7–O20	2.58(1)	Li7–O20	2.42(1)
Li7–O22	1.95(9)	Li7–O22	2.43(1)	Li7–O22	2.63(1)
Li7–H_2O(Cs4)	2.02(6)	Li7–H_2O(Cs4)	2.35(1)	Li7–H_2O(Cs4)	2.42(1)
Li7–H_2O(Cs7)	2.24(13)	Li7–H_2O(Cs7)	2.20(2)	Li7–H_2O(Cs7)	2.05(2)
		Li7–H_2O(Cs7)	2.35(1)	Li7–H_2O(Cs7)	2.43(2)

TABLE 8
Assignment of ^{6}Li MAS NMR Resonances of RUB-29 (As-Synthesized) and Na-3–RUB-29 (Powder)

RUB-29 As-synthesized							Total
Chemical shift (ppm)	1.00	0.89	0.76	0.41	0.18	0.02	
Number of Li cations per unit cell, based on ^{6}Li MAS NMR and chemical analysis	2	3	10	6	18	3	42
Peak assignment	Li7	Li8	Li4	Li5	Li2 + Li3 + Li6	Li1	
Number of Li cations on each site, resulting from neutron data analysis (1)	4	5	8	6	16	3	42
Na–RUB-29 Na-3–RUB-29 (powder)							Total
Chemical shift (ppm)	0.95		0.66		0.25		
Number of Li cations per unit cell, based on ^{6}Li MAS NMR and chemical analysis	1		13		26		40
Peak assignment	Li on Cs6		Li8* + Li4		Li1 + Li2 + Li3 + Li6 + Li5		

resonance at 1.0 ppm, which is reduced in intensity in the spectrum of Na-3–RUB-29, is assigned to Li cations on this site. Interestingly, the least shielded site (i.e., the site with the weakest interaction with framework oxygen atoms) is the site that is ion exchanged.

It is not clear whether the resonance at 0.41 ppm of as-synthesized RUB-29 should be assigned to Li4 or Li5 site, since the structural surroundings for both sites are very similar. Based on consideration of the occupancies of Li4, Li5, and Li8 sites we tentatively assign the resonance at 0.41 ppm in the RUB-29 spectrum to the Li5 site. This assignment is supported by the stronger value of bond valence for Li5 (=0.87) than that for Li4 (=0.81). The remaining resonances at 0.76 ppm of RUB-29 and at 0.66 ppm in the Na form are then, mostly likely, due to Li cations at Li4 and Li8, as summarized in Table 8.

The line broadening of the Na-3–RUB-29 spectrum may be explained by the disturbance of the local environments for the non-framework (Li4 and Li5) and framework Li sites caused by the Na exchange. In particular, the Cs3 site is nearest to the Li sites, of all Cs cations substituted by Na. This line broadening could be also caused by changes in dynamic disorder of Li cations before and after Na exchange. To study the details of the mobility of the Li cations as a function of the type of exchanging cations, a

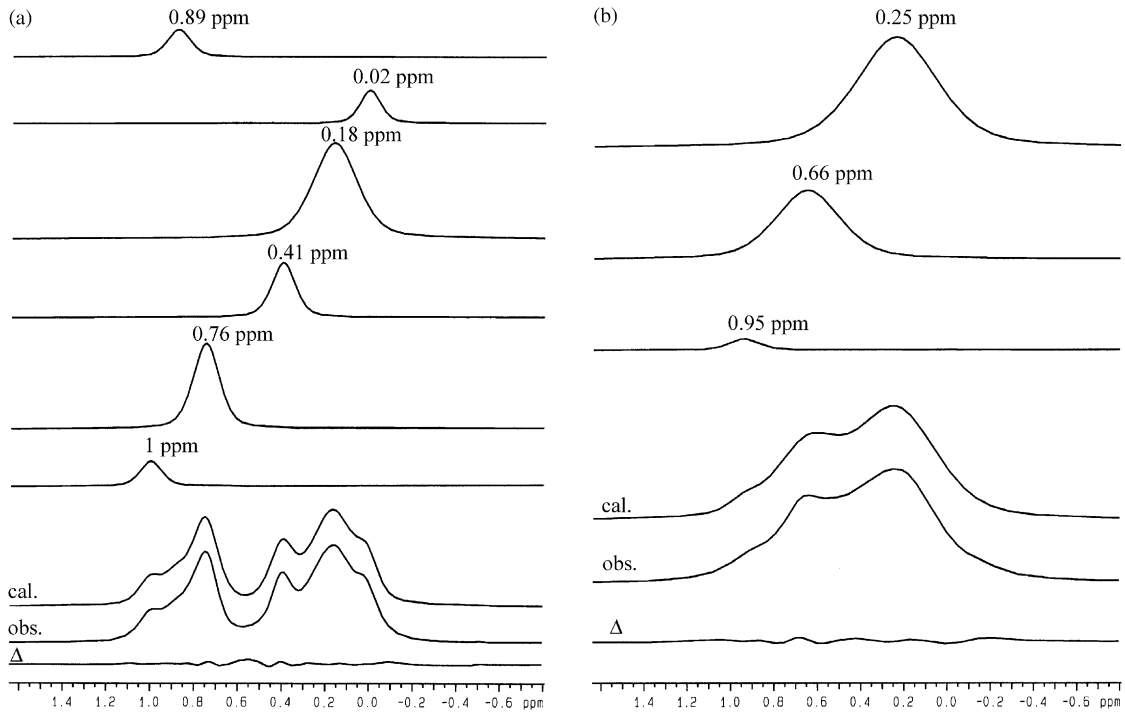

FIG. 6. Deconvolution of ^{6}Li HPDEC MAS NMR spectra of as-synthesized RUB-29 (a) and Na-3–RUB-29 (b). obs.: observed ^{6}Li HPDEC MAS NMR spectrum; cal.: calculated ^{6}Li HPDEC MAS NMR spectrum by deconvolution; Δ: (obs−cal). Individual resonances with their chemical shifts are extra plotted above each calculated spectrum (cal.).

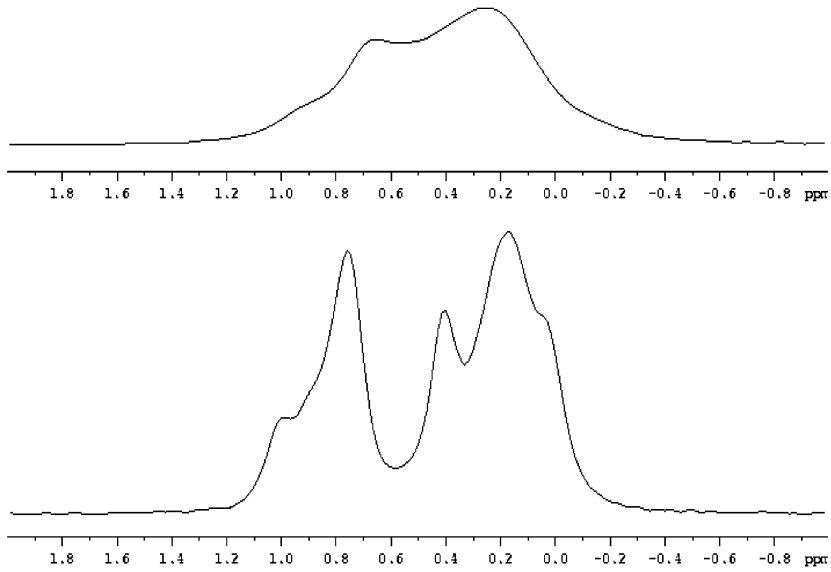

FIG. 7. Comparison of the ^{6}Li HPDEC MAS NMR spectra of as-synthesized RUB-29 (bottom) and of Na-3–RUB-29 (top). Resonances at lower chemical shifts are assigned to framework Li cations and the others to non-framework Li cations.

series of variable temperature ^{6}Li NMR experiments are in progress.

The discrepancy between the numbers of Li cations calculated from ^{6}Li NMR and those from structure analysis can be explained by a non-negligible uncertainty of the amount of Li determined from chemical analysis. The low scattering power of Li makes accurate characterization difficult, and static and dynamic disorder further complicates crystallographic study. However, the presence of clearly resolved ^{6}Li NMR resonances for the RUB-29 structures before and after Na exchange allows resolution of framework and non-framework Li cations for the first time using ^{6}Li NMR techniques. The chemical shifts of the Li resonances are clearly extremely sensitive to the ion-exchange process.

CONCLUSION

The combined results of synchrotron X-ray single-crystal diffraction and ^{6}Li MAS HPDEC NMR spectroscopy allowed for a better understanding of the complex behavior of RUB-29 structure upon Na exchange. This exchange process involved seven Cs- and four Li sites of RUB-29. The ease with ion exchangeability in the complicated channel system was predicted in terms of bond valence and accessibility for these Cs and Li cation sites. Sodium cations can exchange with more than 90% of the Cs cations and 16% of the Li cations without resulting in any changes in the lattice symmetry. Most Li cations within the channels either remain or relocate. The successful removal of Cs and its replacement by the smaller sodium suggests that the interior of RUB-29 may be made available for possible gas separation applications.

To determine more exact Li positions and their occupancies, it is necessary to investigate dehydrated forms of Na–RUB-29 using high-resolution neutron diffraction data. We have conducted neutron powder diffraction experiments of dehydrated Na–RUB-29 and data analyses are in progress. It is hoped these data will allow a more detailed investigation of the relationship between the behavior of non-framework and framework Li cations and changes in framework geometry as a function of the degree of ion exchange.

ACKNOWLEDGMENTS

We acknowledge financial support from the NSF and the DOE via DMR-0095633 (JBP), DEFG0296ER14681 (CPG), and DBI-9907840 (NMR). We thank Dr. Peter J. Eng and Prof. Joseph J. Pluth (GESCARS, University of Chicago, IL, USA) for support in collecting single crystal synchrotron X-ray data of Na–RUB-29 samples at the beam line GESCARS at APS. This work was supported by DOE grant DE-FGO2-94ER14466, NSF grant EAR-9906456, and the W. M. Keck foundation (GSECARS). Use of the Advanced Photon Source was supported by the DOE, BES, Office of Energy Research, under Contract No. W-31-109-ENG-38. Dr. Martine Ziliox (Structural Biology, SUNY at Stony Brook, NY, USA) and Dr. Haiming Liu helped us to obtain ^{6}Li MAS HPDEC NMR spectra.

REFERENCES

1. S.-H. Park, J. B. Parise, H. Gies, H. Liu, C. P. Grey, and B. H. Toby, *J. Am. Chem. Soc.* **122**(44), 11,023–11,024 (2000).

2. S.-H. Park, J. B. Parise, and H. Gies, "Proceedings of the 13th International Zeolite Conference, Montpellier, France, 8–13 July, 2001. Studies in Surface Science and Catalysis," Vol. 135 (A. Galarneau, F. Di Renzo, F. Fajula, and J. Vedrine, Eds). Elsevier Science, Amsterdam, 2001.
3. Y. Lee, S. W. Carr, and J. B. Parise, *Chem. Mater.* **10,** 2561–2570 (1998).
4. Y. Lee, C. Cahill, J. Hanson, J. B. Parise, S. Carr, M. L. Myrick, U. V. Preckwinkel, and J. C. Phillips, "Proceedings of the 12th International Zeolite Association Meeting, Baltimore, Maryland, July 5–10, 1998" (M. M. J. Treacy, B. K. Marcus, M. E. Bisher, and J. B. Higgins, Eds), Vol. IV, pp. 2401–2408. Materials Research Society (Vols. I–IV), MRS, Warrendale, PA, 1999.
5. Y. Lee, S.-J. Kim, M. A. Schoonen, and J. B. Parise, *Chem. Mater.* **12,** 1597–1603 (2000).
6. J. B. Parise, C. Cahill, and Y. Lee, *Can. Mineral.* **38,** 777–800 (2000).
7. I. D. Brown, "Structures and Bonding in Crystals" (M. O'Keeffe and A. Navrotsky, Eds), Chap. 14. Academic Press, New York, 1981.
8. I. D. Brown and R. D. Shannon, *Acta Crystallogr. A* **29,** 266–282 (1973).
9. M. Feuerstein, G. Engelhardt, P. L. McDaniel, J. E. MacDougall, and T. R. Gaffney, *Micropr. Mesopr. Mater.* **26,** 27–35 (1998).
10. S. Ramírez, J. M. Domínguez, M. Viniegra, and L. C. de Ménorval, *New J. Chem.* **24,** 99–104 (2000).
11. D. Forano, R. C. T. Slade, E. Krogh Anderson, I. G. Krogh Anderson, and E. Price, *J. Solid State Chem.* **82,** 95–102 (1996).
12. J. F. Stebbins, Z. Xu, and D. Vollath, *Solid State Ionics* **78,** L1–L8 (1995).
13. M. Feuerstein and R. F. Lobo, *Chem. Mater.* **10**(8), 2197–2204 (1998).
14. M. Feuerstein and R. F. Lobo, *J. Chem. Soc. Chem. Commun.* 1647–1648 (1998).
15. S.-H. Park, P. Daniels, and H. Gies, *Micropr. Mesopr. Mater.* **37,** 129–143 (2000).
16. S.-H. Park, M. Kleinsorge, H. Liu, C. P. Grey, and J. B. Parise, "Abstracts for Recent Research, 13th International Zeolite Conference, Montpellier, France, 8–13 July 2001."
17. Bruker Analytical X-ray Systems, "SMART (version 5.0, 1997), SAINT (version 4, 1994–1996) including SADABS, and SHELXTL (version 5.10, 1998) for Windows NT®."
18. J. Stolz, P. Yang, and Th. Armbruster, *Micropr. Mesopr. Mater.* **37,** 233–242 (2000).
19. D. H. Olson, *Zeolites* **15,** 439–443 (1995).